MicroED

April 4, 2018

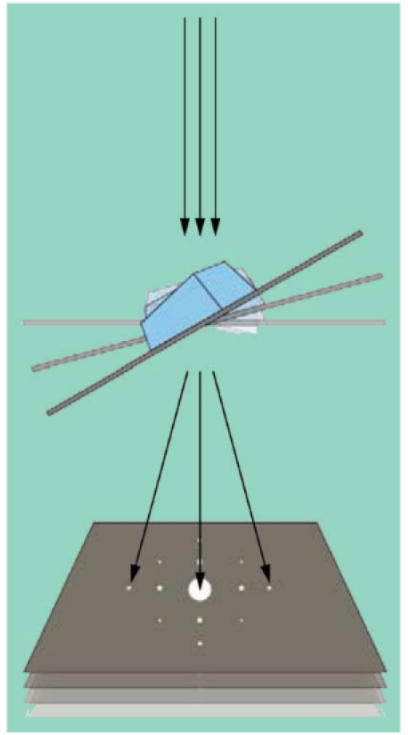

Best Resolution from EM Techniques

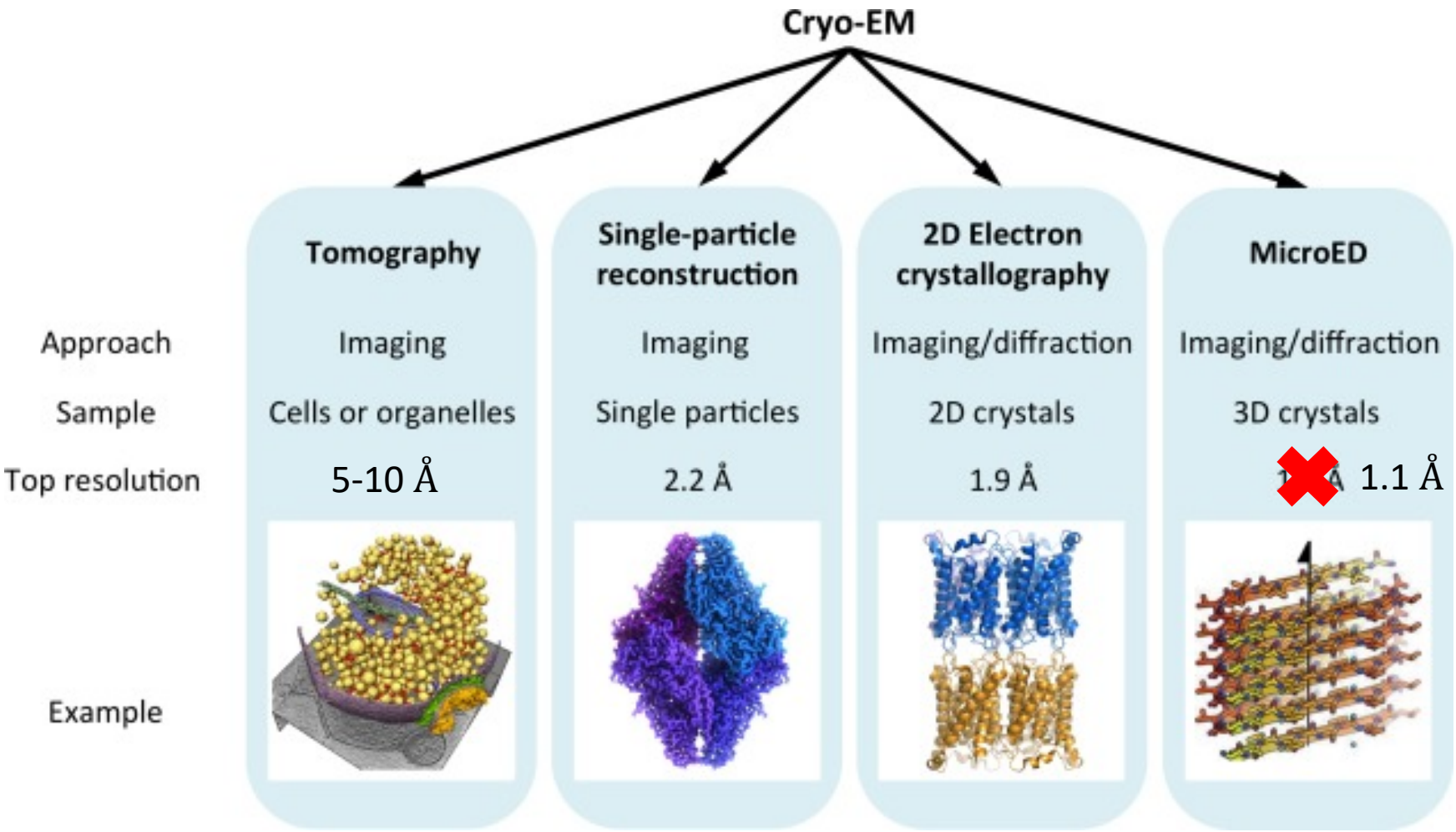

Structures Solved by MicroED

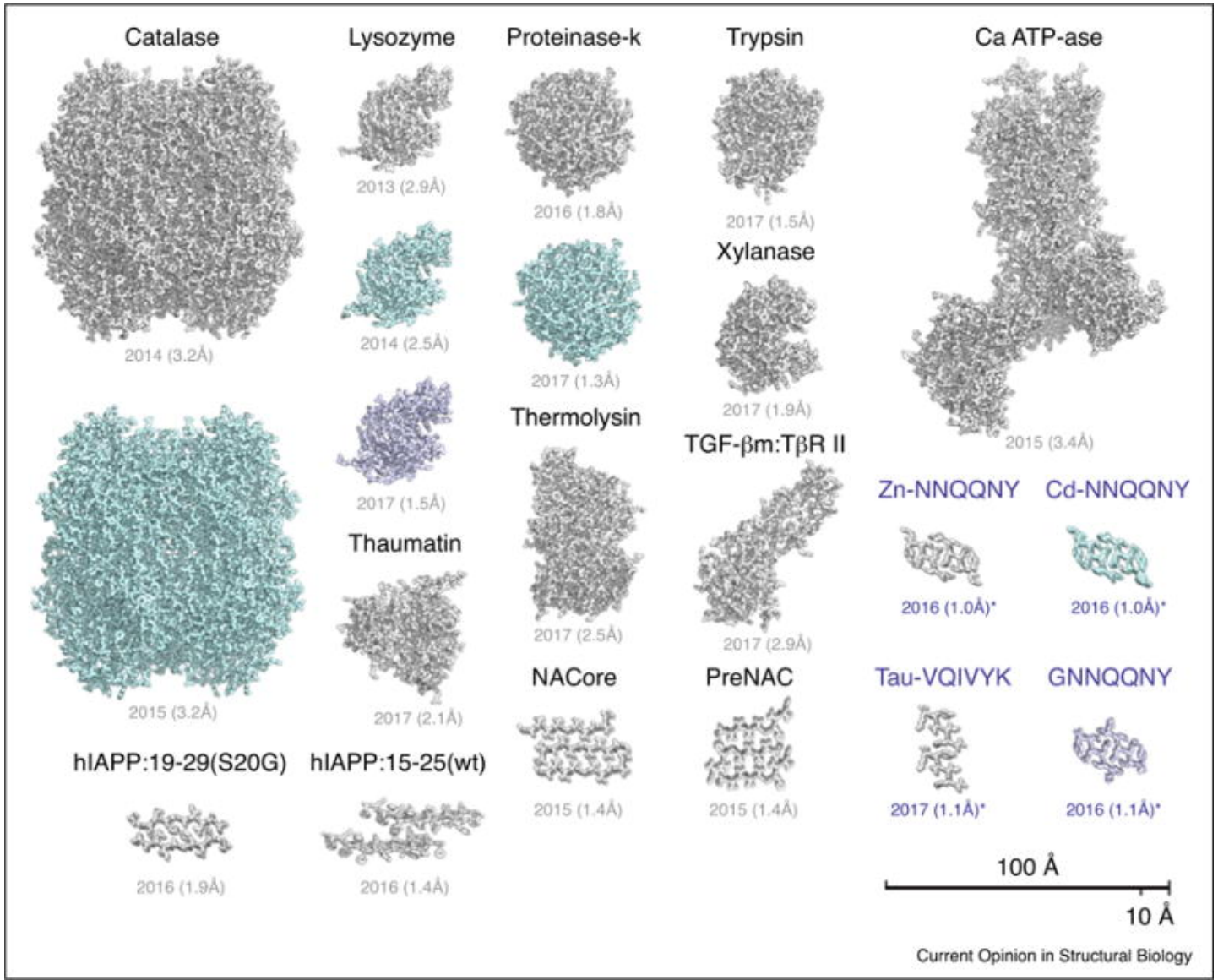

Curr Opin Struct Biol. 2017 Oct; 46: 79–86.

Structures Solved by MicroED

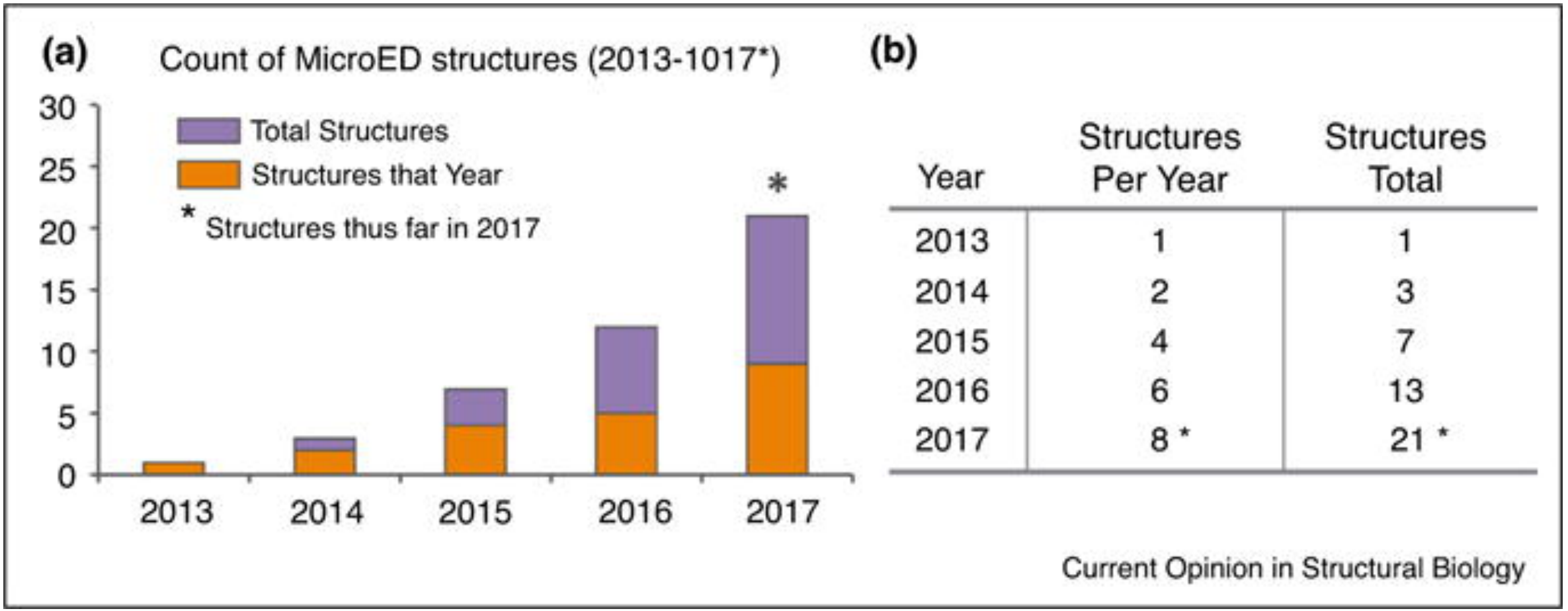

(b)

Year	Structures Per Year	Structures Total
2013	1	1
2014	2	3
2015	4	7
2016	6	13
2017	8 *	21 *

Current Opinion in Structural Biology

EMDB Released Entries

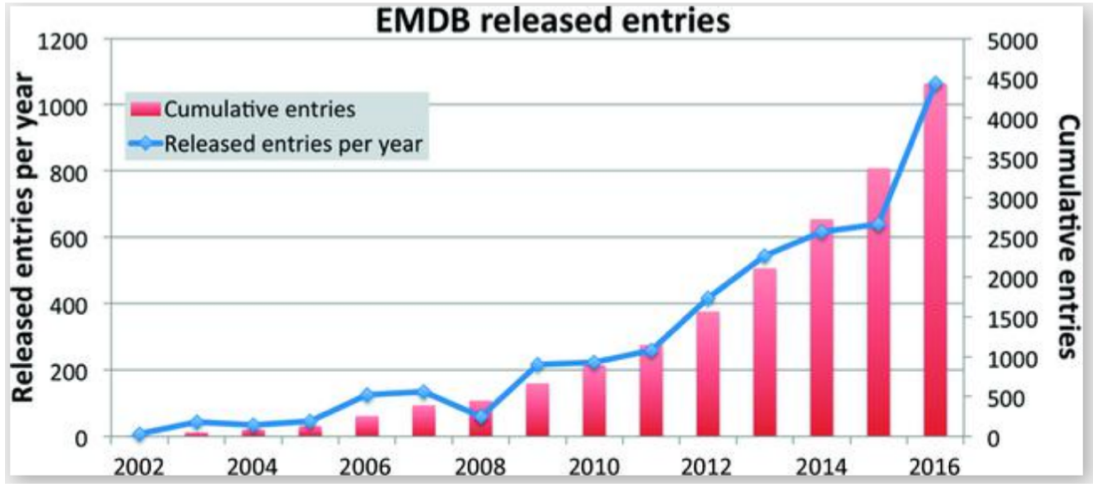

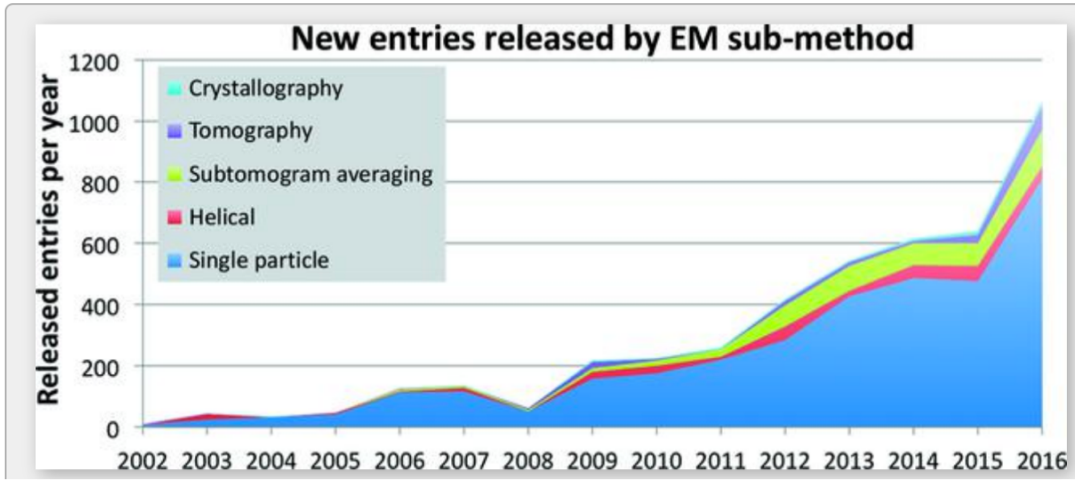

https://doi.org/10.1107/S2059798317004181

Structures Solved by MicroED

Sample	PDB code	R_{work} | R_{free} (%)	Ref	Phasing method	Res. (Å)	Space group	Cell dimensions a, b, c (Å) | α, β, γ (°)
Lysozyme	3J4G	25.5 | 27.8	[7••]	MR	2.9	P 4_3 2_1 2	77, 77, 37 | 90, 90, 90
Lysozyme	3J6K	22.0 | 25.5	[8••]	MR	2.5	P 4_3 2_1 2	76, 76, 37 | 90, 90, 90
Lysozyme	5K70	23.9 | 28.4	[36••]	MR	1.5	P 4_3 2_1 2	76, 76, 37 | 90, 90, 90
Catalase	3J7B	26.2 | 30.8	[10•]	MR	3.2	P 2_1 2_1 2_1	68, 172, 182 | 90, 90, 90
Catalase	3J7U	27.2 | 31.7	[11•]	MR	3.2	P 2_1 2_1 2_1	69, 174, 206 | 90, 90, 90
Ca-ATPase	3J7T	27.7 | 31.5	[11•]	MR	3.4	C 2	166, 64, 147 | 90, 98, 90
Proteinase K	519S	19.7 | 25.6	[9•]	MR	1.8	P 4_3 2_1 2	67, 67, 102 | 90, 90, 90
Proteinase K	5K7S	22.4 | 25.5	[36••]	MR	1.3	P 4_3 2_1 2	67.6, 67.6, 101.4 | 90, 90, 90
Thermolysin	5K7T	28.7 | 30.6	[36••]	MR	1.6	P 6_1 2 2	90.8, 90.8, 126 | 90, 90, 120
Trypsin	5K7R	24.8 | 28.1	[36••]	MR	1.5	P 2_1 2_1 2_1	53.1, 56.1, 64.4 | 90, 90, 90
Thaumatin	5K7Q	24.5 | 29.2	[36••]	MR	2.1	P 4_1 2_1 2	57.8, 57.8, 150 | 90, 90, 90
Xylanase	5K7P	22.1 | 26.2	[36••]	MR	1.9	P 2_1 2_1 2_1	49.1, 59, 70 | 90, 90, 90
TGFβ:TβRII	5TY4	29.2 | 32.8	[36••]	MR	2.9	P 2_1 2_1 2_1	41.5, 71.3, 79.5 | 90, 90, 90
NACore	4RIL	24.8 | 27.5	[14••]	MR	1.4	C 2	70.8, 4.8, 16.8 | 90, 106, 90
PreNAC	4ZNN	23.5 | 28.2	[14••]	MR	1.4	P 2_1	17.9, 4.7, 33 | 90, 94, 90
hIAPP 19-29 (S20G)	5KNZ	22.8 | 27.5	[35•]	MR	1.9	P 2_1 2_1 2_1	4.8, 18.6, 70.8 | 90, 90, 90
hIAPP 15-25 (WT)	5KO0	22.4 | 25.9	[35•]	MR	1.4	P1	11.7, 18.2, 19.9 | 63, 89, 88
Tau (VQIVYK)	5K7N	21.0 | 22.4	[36••][a]	DM	1.1	C 2	29.3, 4.97, 37.6 | 90, 112, 90
Sup35 (Zn-NNQQNY)	5K2E	15.6 | 19.4	[12••][a]	DM	1.0	P 2_1	21.5, 4.9, 23.9 | 90, 104, 90
Sup35 (Cd-NNQQNY)	5K2F	22.0 | 24.2	[12••][a]	DM	1.0	P 2_1	22.1, 4.9, 23.5 | 90, 104, 90
Sup35 (GNNQQNY-1)	5K2G	18.7 | 22.4	[12••][a]	DM	1.1	P 2_1	22.9, 4.9, 24.2 | 90, 108, 90
Sup35 (GNNQQNY-2)	5K2H	17.7 | 18.6	[12••][a]	DM	1.05	P 2_1 2_1 2_1	23.2, 4.9, 40.5 | 90, 90, 90

Sample Structures

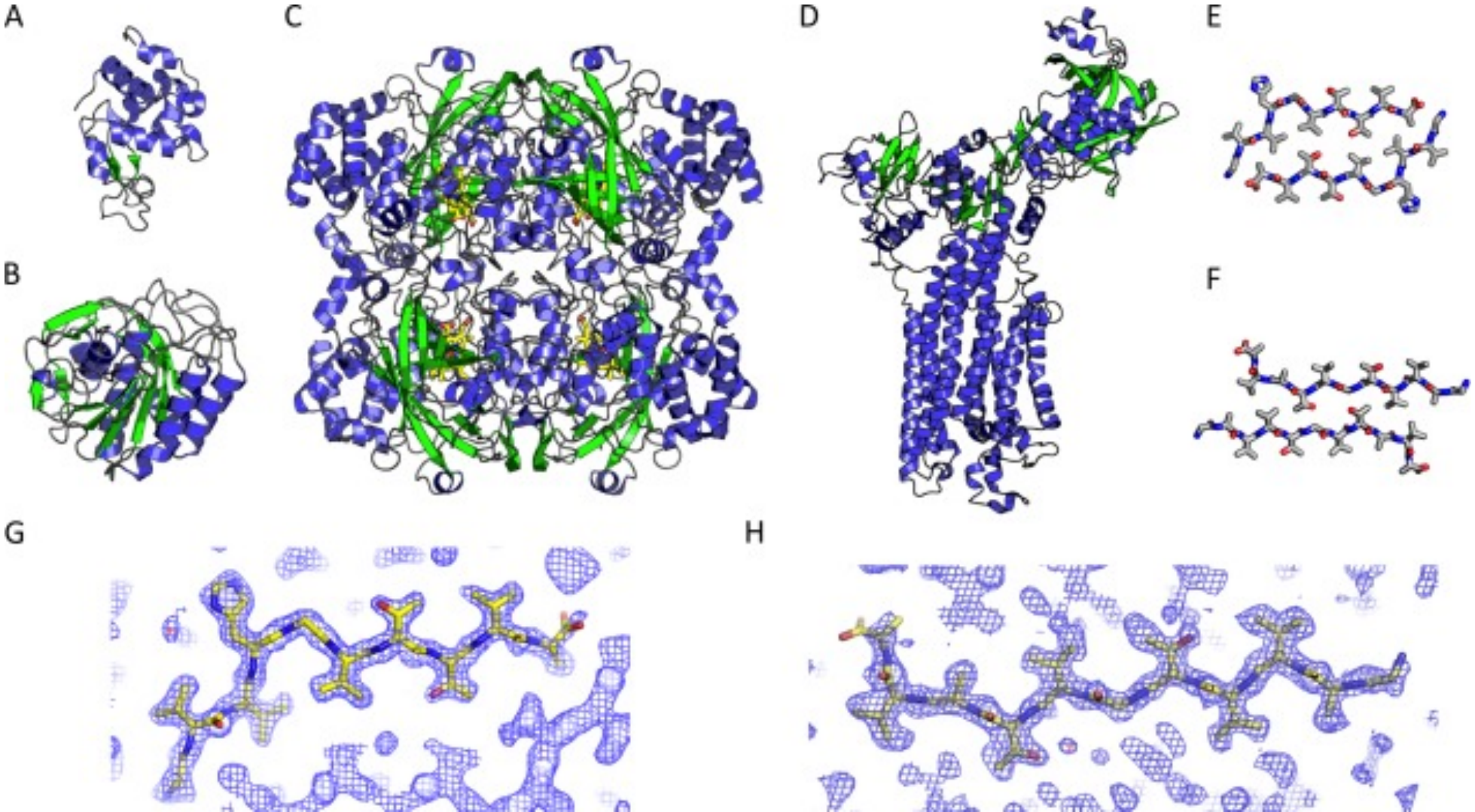

Toxic core of a-synuclein from invisible crystals

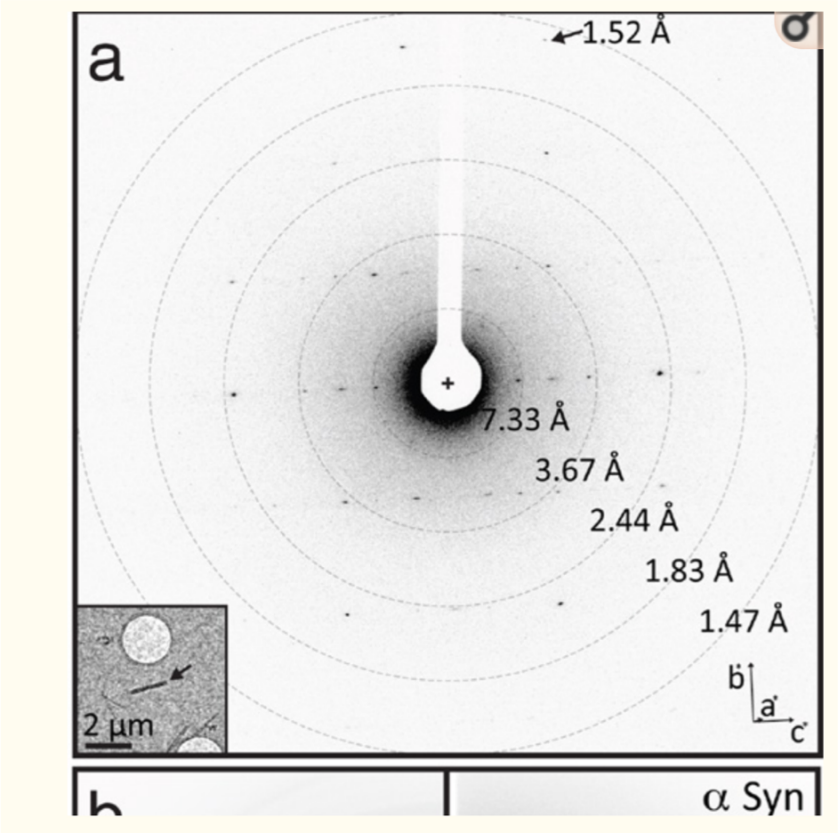

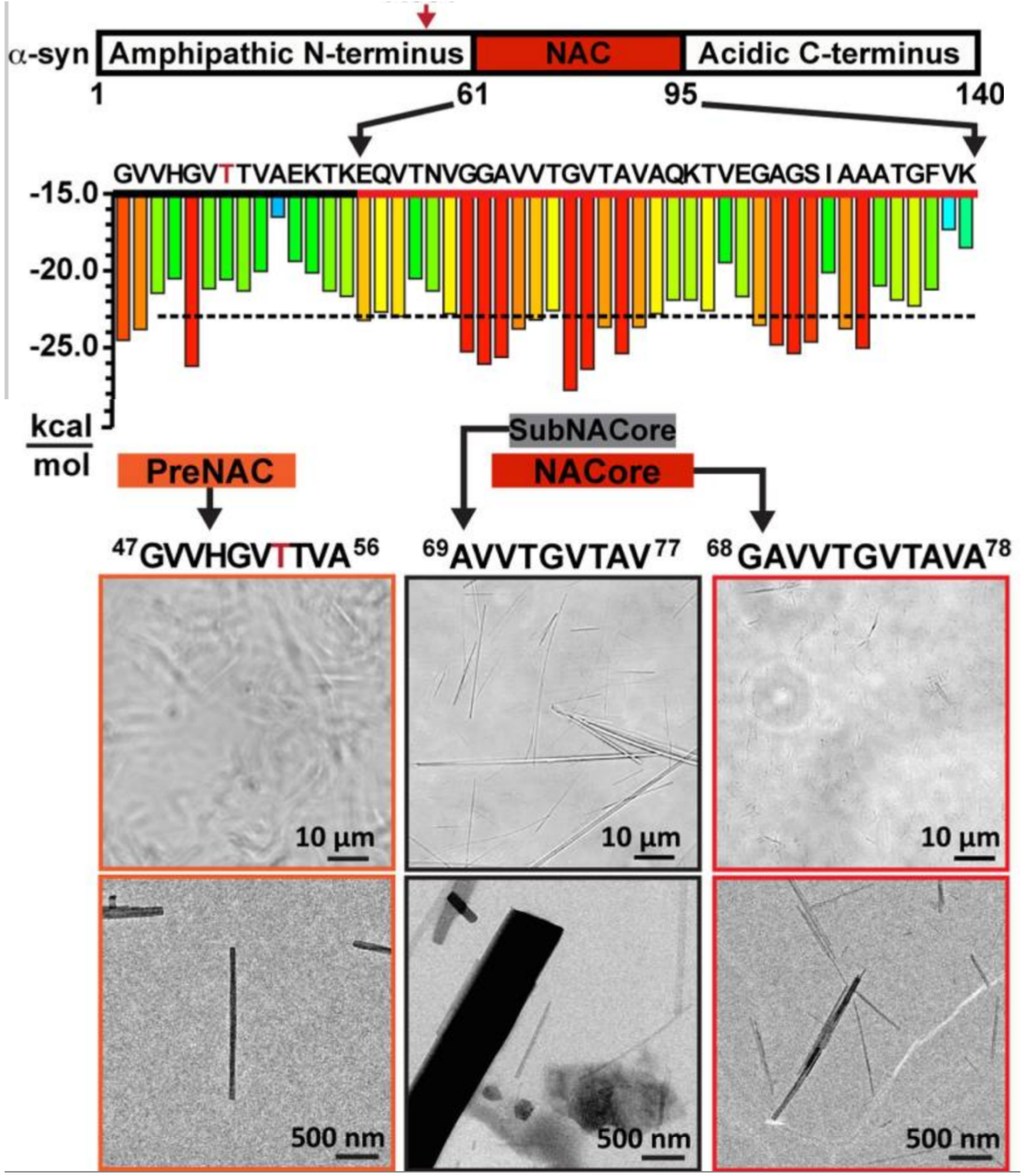

Structure of Amyloid core

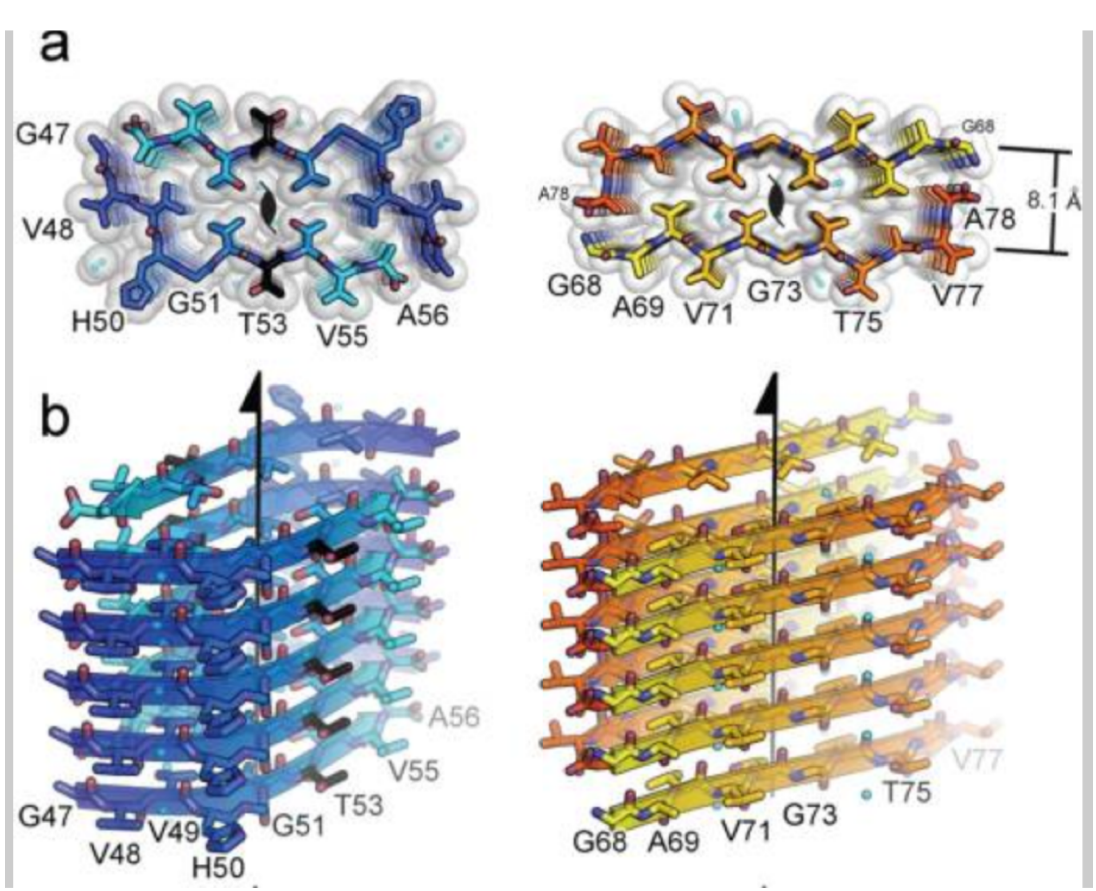

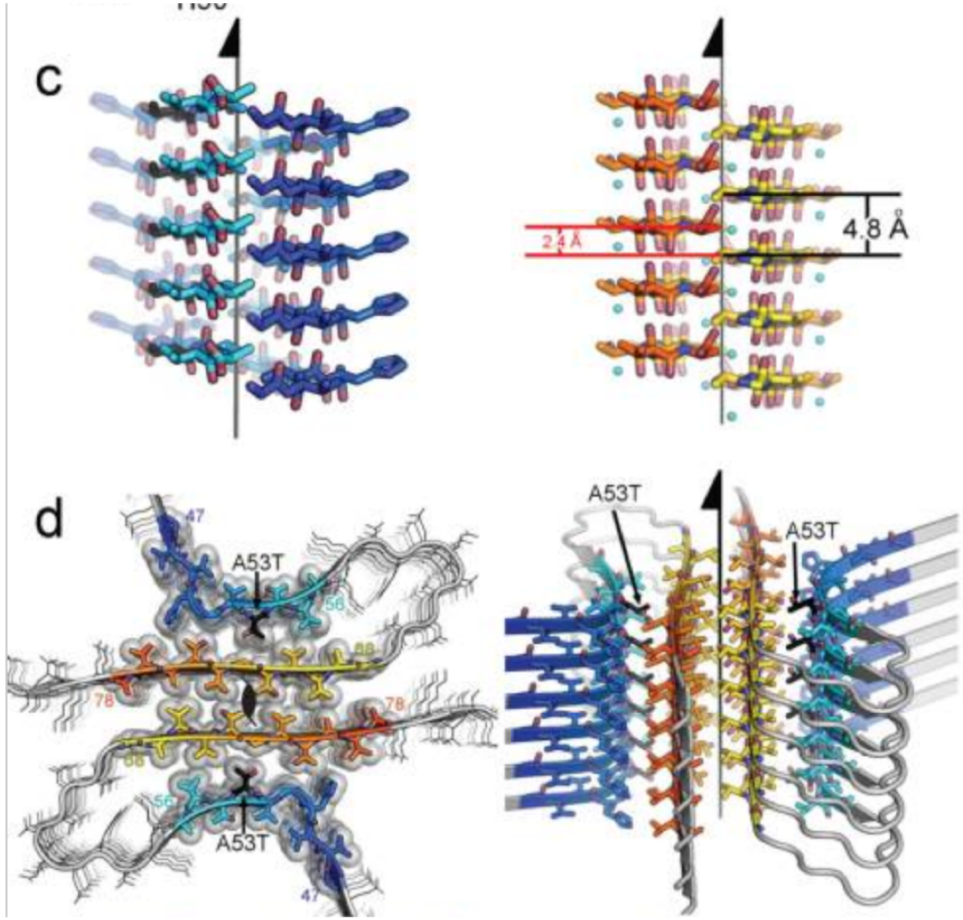

Brief review of X-ray crystallography

Diffraction Review

- Set of scattering points separated by distance d
- Beam hits at angle θ relative to plane
- Constructive interference only when their path length difference keeps them in phase
- Bragg's law
  - $n\lambda = 2d \sin \theta$

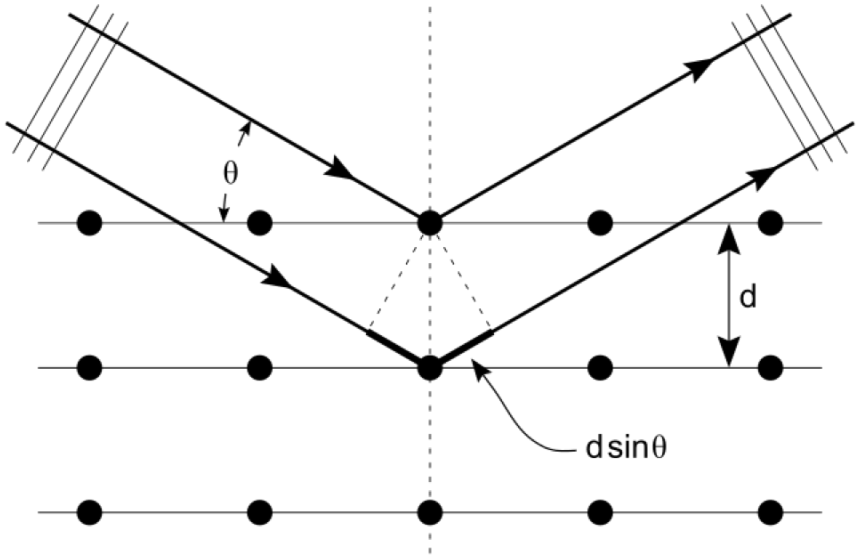

X-Ray Diffraction

- Mount crystal, expose to x-ray beam at defined wavelength
- Collect images of reflections on detector
- Only collect intensities and positions, not phases
- Rotate crystal (180 deg) to get all reflections
- From positions, get 3D lattice parameters
- Phasing
  - Ab initio (small, high resolution)
  - Heavy atom derivatives
  - MAD/SAD
  - Molecular replacement

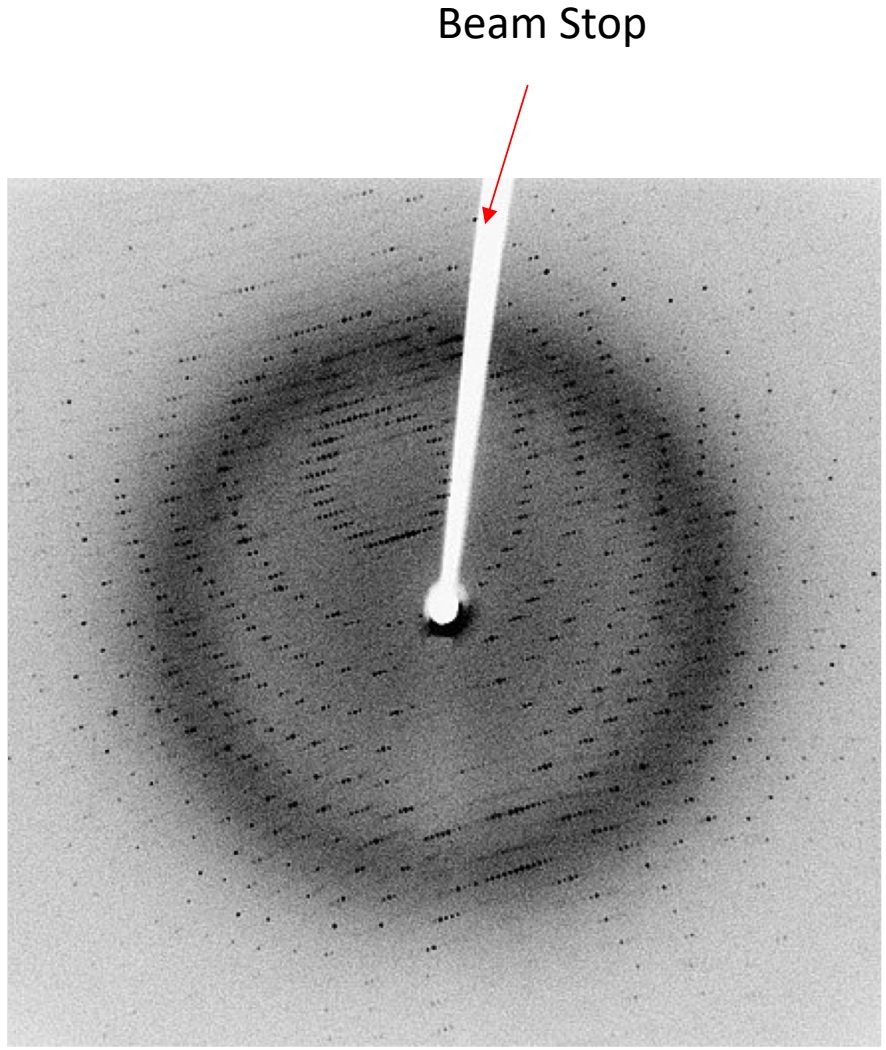

Ewald Sphere

- Sphere of radius 1/λ surrounding the crystal
- Only see diffraction spots which intersect the sphere
- For different wavelengths, get a differently sized sphere
- Rotate crystal on the beam to see different spots
- Xray:
  - λ=0.709 Å (Ag Ka)
  - Λ=1.54 Å (Cu Ka)

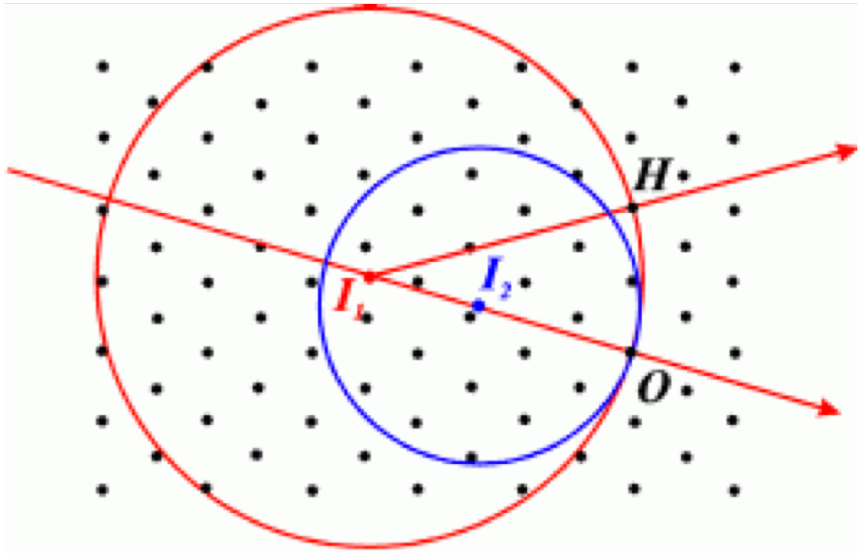

Figure 2

Ewald Sphere

- If you rotate the crystal, the sphere rotates about the origin O
- Yellow area is swept out
- Only observe reflections in the yellow area

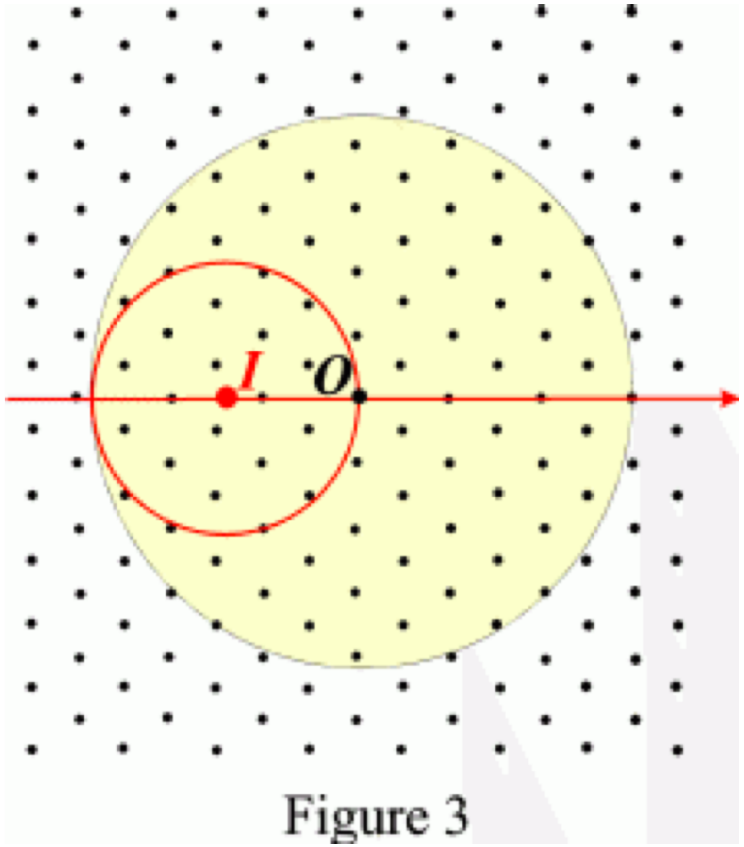

Figure 3

Oscillation Method

Still Image

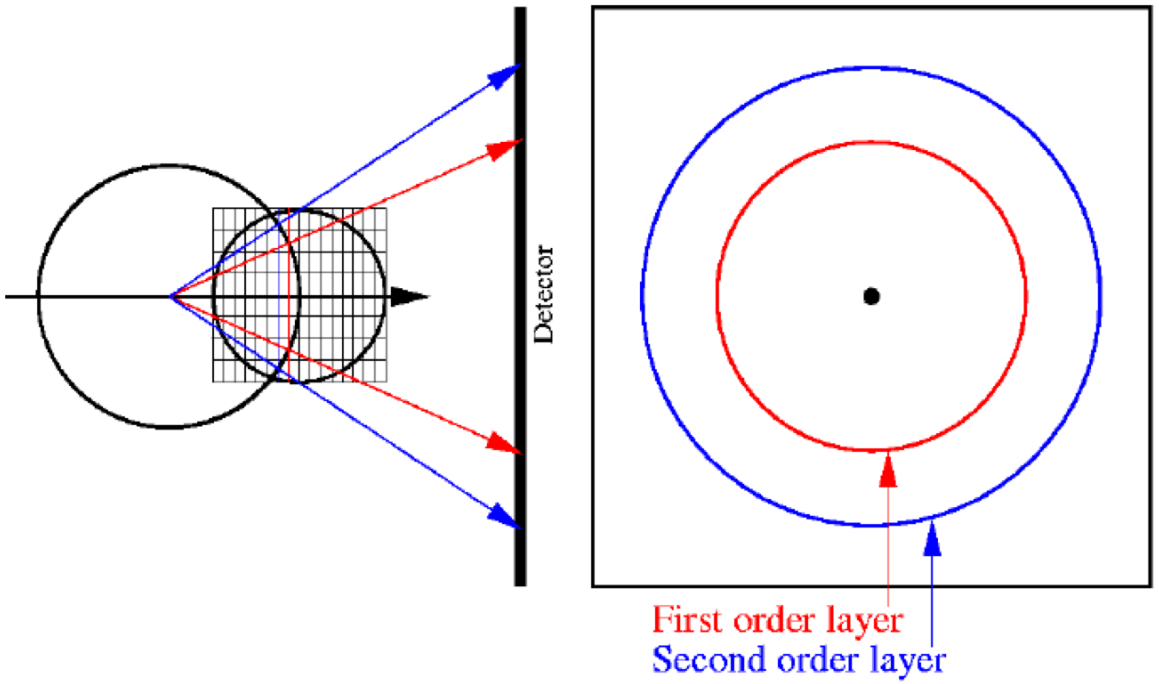

Oscillating Image

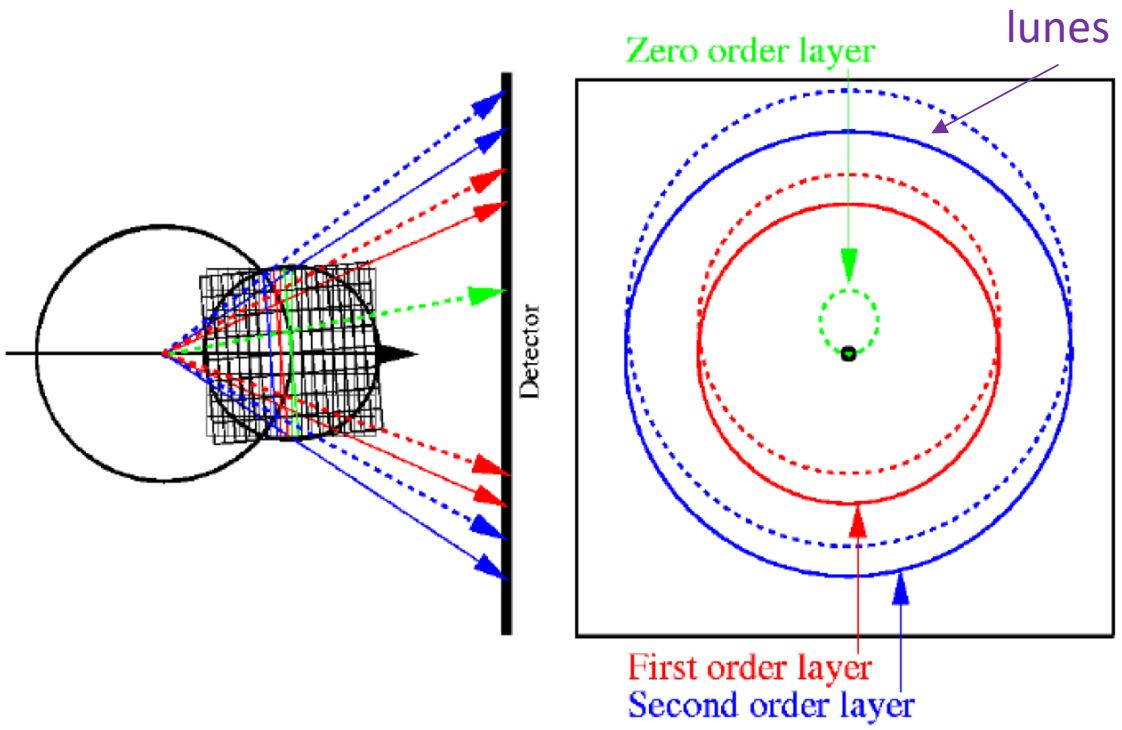

Oscillation method

Image 1

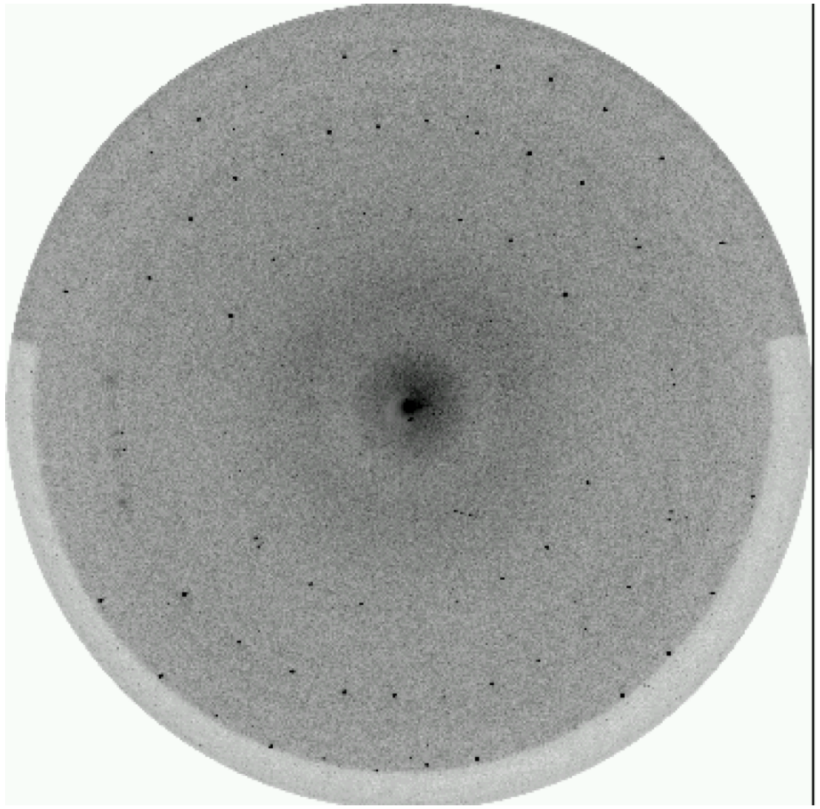

Rotate crystal 5 degrees, oscillate 0.5 degrees

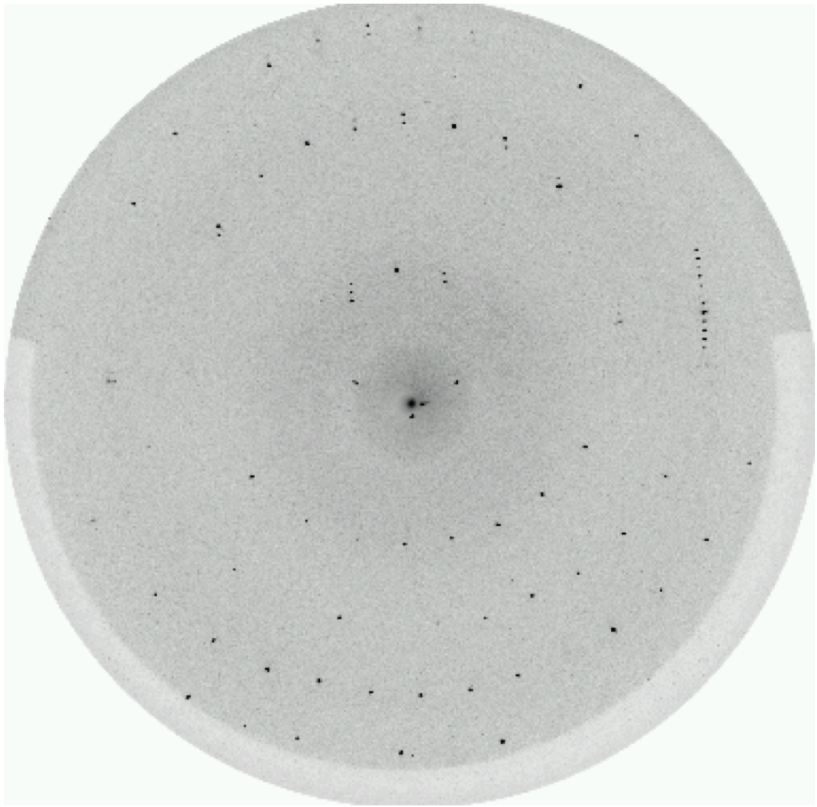

Limitations of X-ray crystallography

- Approximately 30% of proteins that crystallize do not produce crystals large enough for x-ray diffraction experiments
  - Rupp, 2004; Quevillon-Cheruel et al., 2004
- XFEL?
  - Need many crystals
  - Expensive experiment

Back to EM

Wavelengths

- X-ray
  - λ=70.9 pm (Ag Ka)
  - λ =154 pm (Cu Ka)

- EM
  - 80 keV: 4.18 pm
  - 120 keV: 3.35 pm
  - 200 keV: 2.51 pm
  - 300 keV: 1.97 pm

Standard Optics

Objective aperture inserted

No SA aperture

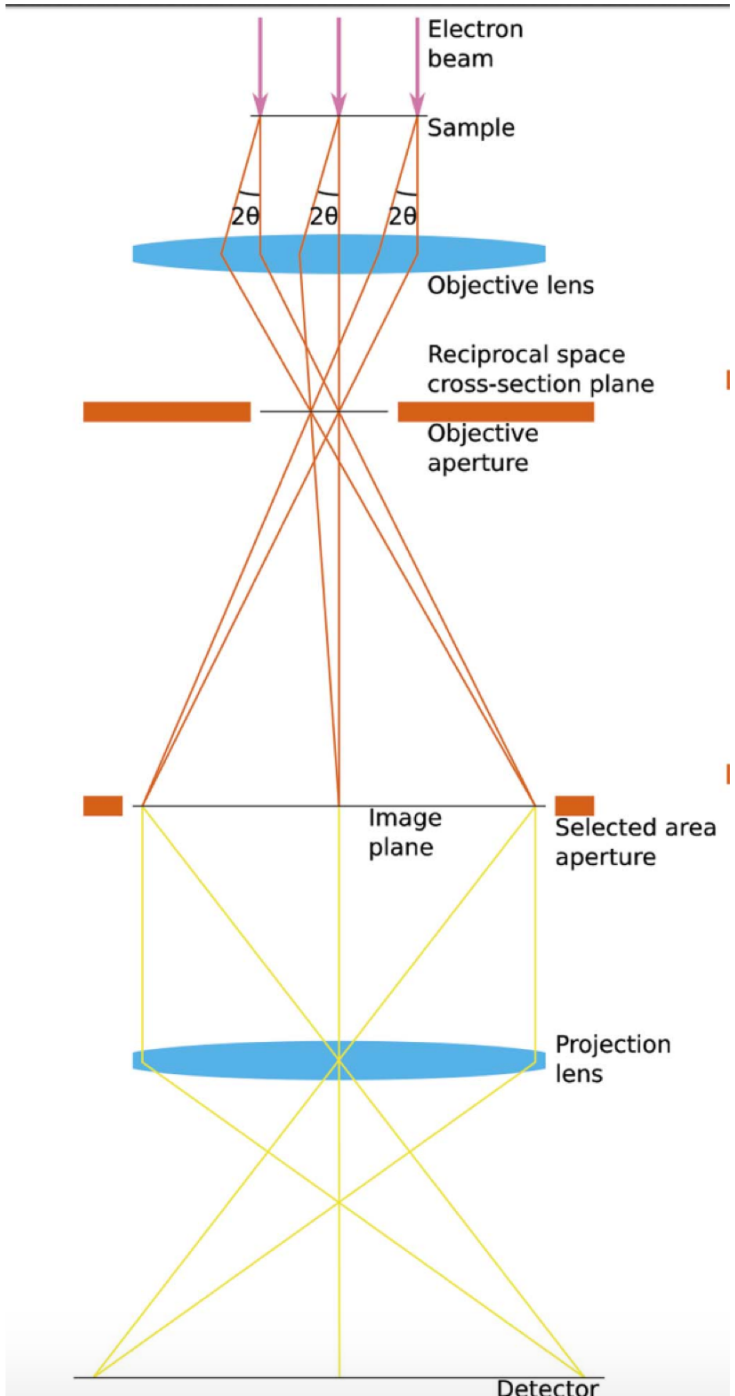

Diffraction Optics

No objective aperture

SA aperture inserted

Beamstop to block direct beam

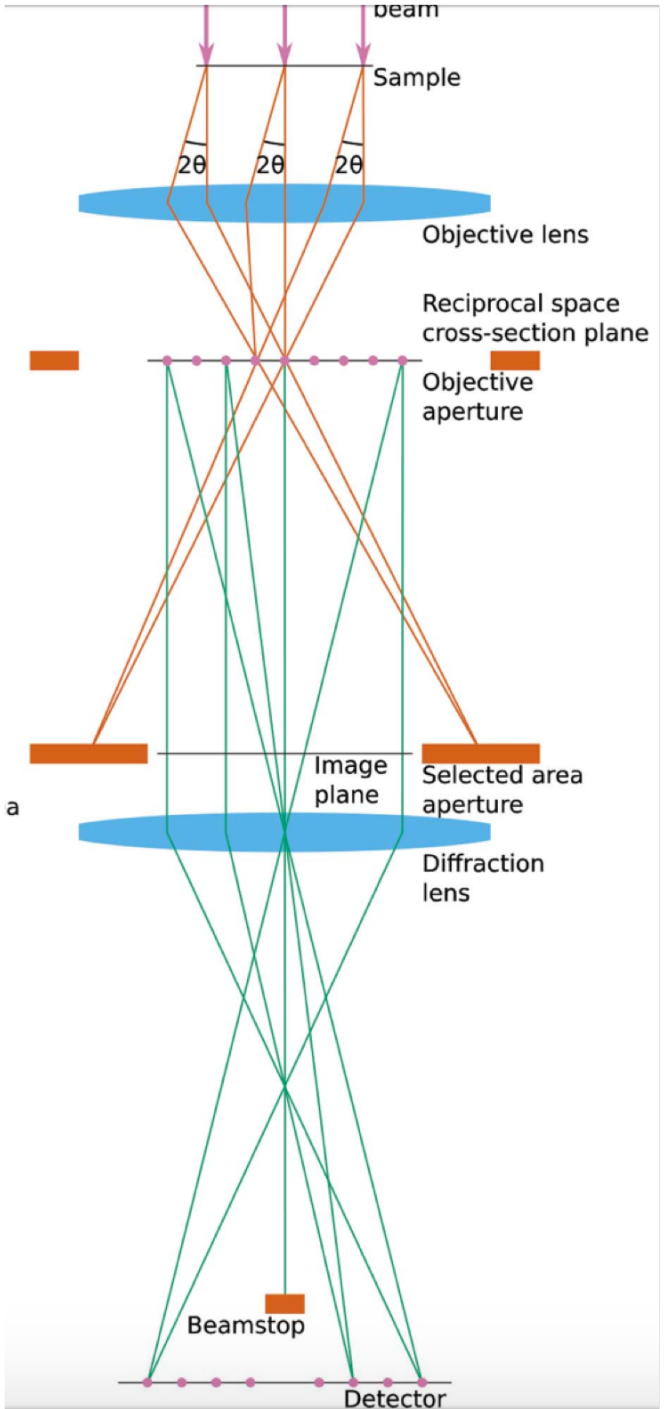

Modes of Collection

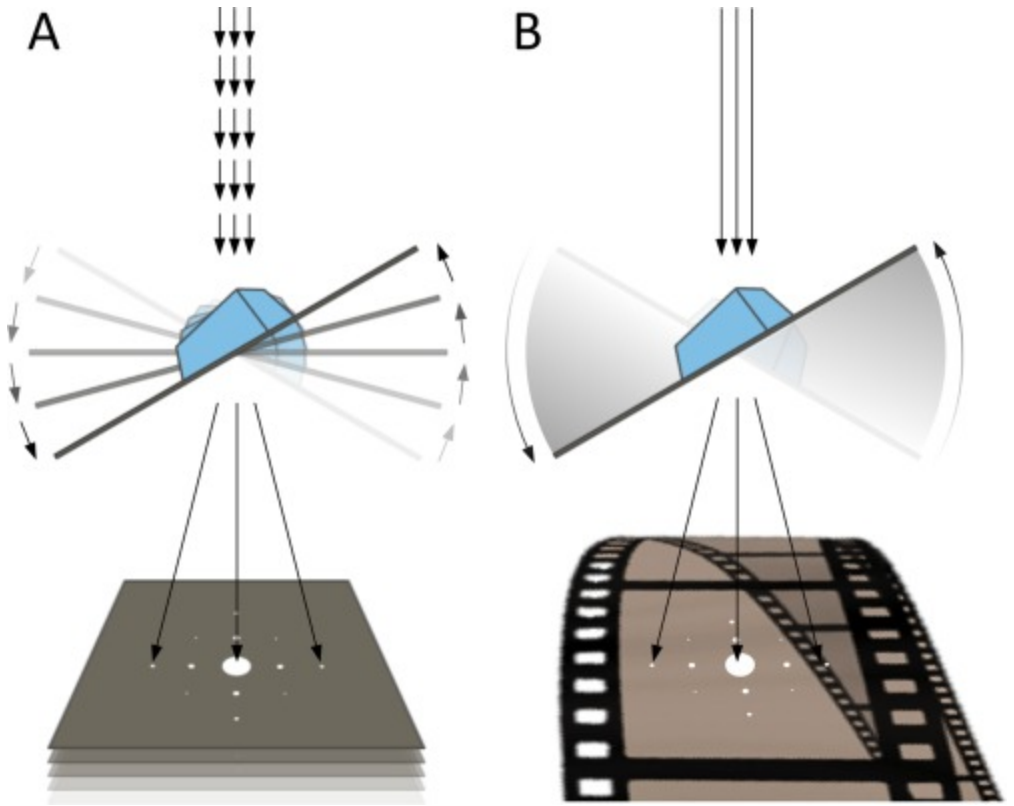

Missing Wedge (-70 to +70 degrees)

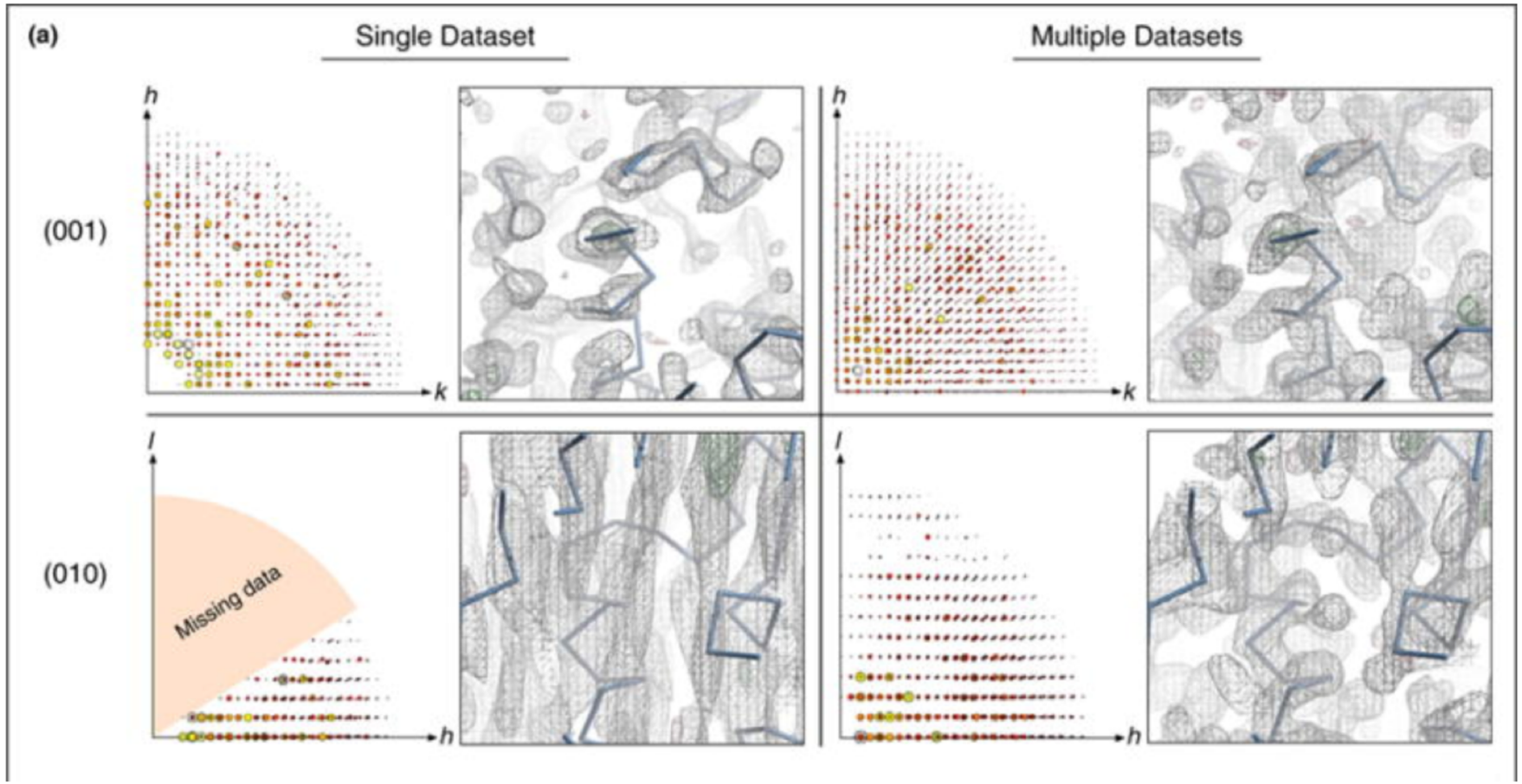

Crystal Thickness

- Diffuse scattering: caused by partial disorder within crystal, as well as inelastic scattering
  - Increased background noise, errors in measurement of intensity levels
- Dynamic scattering: when inelastically scattered electrons have a second scattering effect
  - Intensities meant for a specific reflection are redistributed to other ones, leasing to inaccuracies of integrated reflection counts
- Lysozyme: crystals thicker then 500 nm unusable
  - Maximum thickness may depend on packing and density

Larger (imperfect) crystals

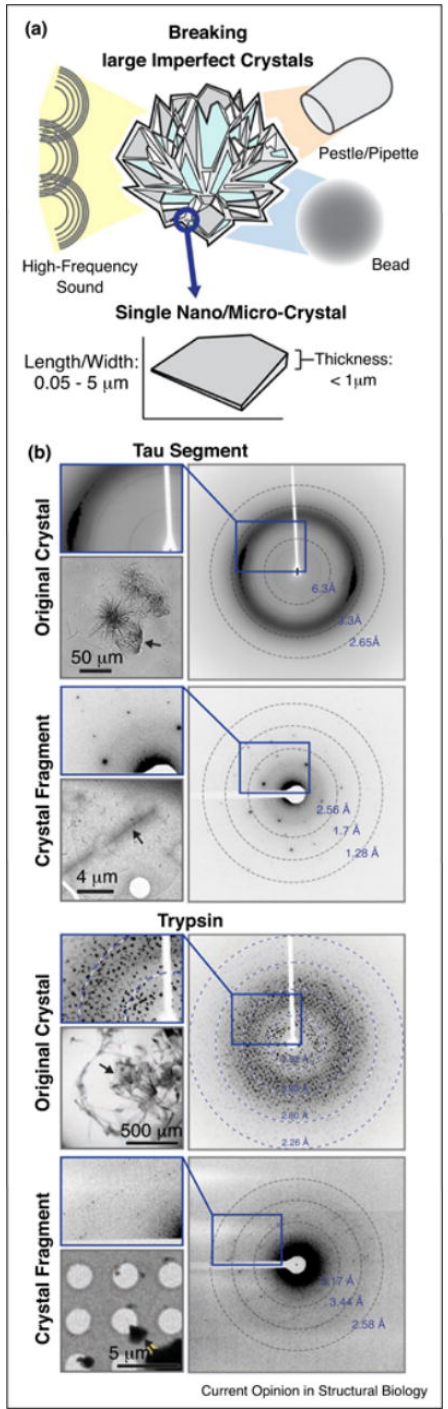

Details

Workflow Overview

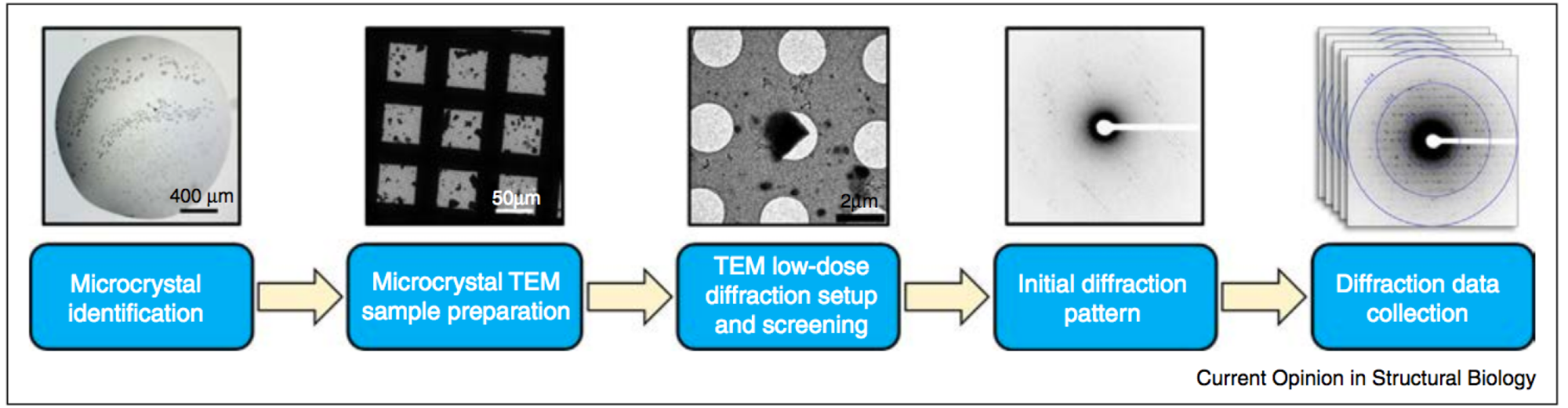

Collection Setup: Initial screen

- Screen by negative stain for crystals
- Plunge freeze
  - Screen for optimal conditions to preserve crystals and have proper ice thickness
- Align microscope for low-dose electron diffraction
  - Optics well aligned for diffraction mode, diffraction astigmatism corrected
- Eucentric sample
- Screen at low mag (100X) for location of crystals and relative ice thickness
- Dose minimal: $<10^{-6}$ $e^{-}Å^{2}s^{-1}$

Collection Setup: Crystal

- Examine crystals in over-focused diffraction mode
  - High contrast imaging at low dose: $<10^{-3}$ $e^{-}Å^{2}s^{-1}$
- Finely tune eucentricity at crystal location
- Set up diffraction: direct beam centered and blocked by beam stop
  - Dose rate 0.01-0.05 $e^{-}Å^{2}s^{-1}$
  - Beam 5-10 µm diameter
  - No objective aperture
  - Selected Area (SA) aperture inserted, approximately size of crystal
- Collect image: 2-5s
- If high quality diffraction seen: collect tilting data set

Data Collection: Single Images

- Single images (like tomography)
- Discrete angles (0.5-1 degree increment)
- Can adjust exposure time depending on diffraction strength
- CMOS camera at best operating condition: enough time to re-charge electronics for each pixel, best signal to noise ratio
- BUT
- Due to Ewald sphere, most reflections are only partially recorded
- Need to either sum the partial observations or figure out what is the full intensity reflection
- Need special software for this processing

Original implementation (Shi et al, 2013)

- Image single images at various tilts (1 deg increment)
  - Oscillation generally used in x-ray crystallography
- Reflections recorded in this manner are generally partial reflections
  - Needed in-house scripts to index the data and group symmetry-related reflections
- Lysozyme at 2.9 Å resolution
  - 200 keV on TVIPS F416 CMOS detector

Three-dimensional electron crystallography of protein microcrystals.
Elife 2013 Nov 19

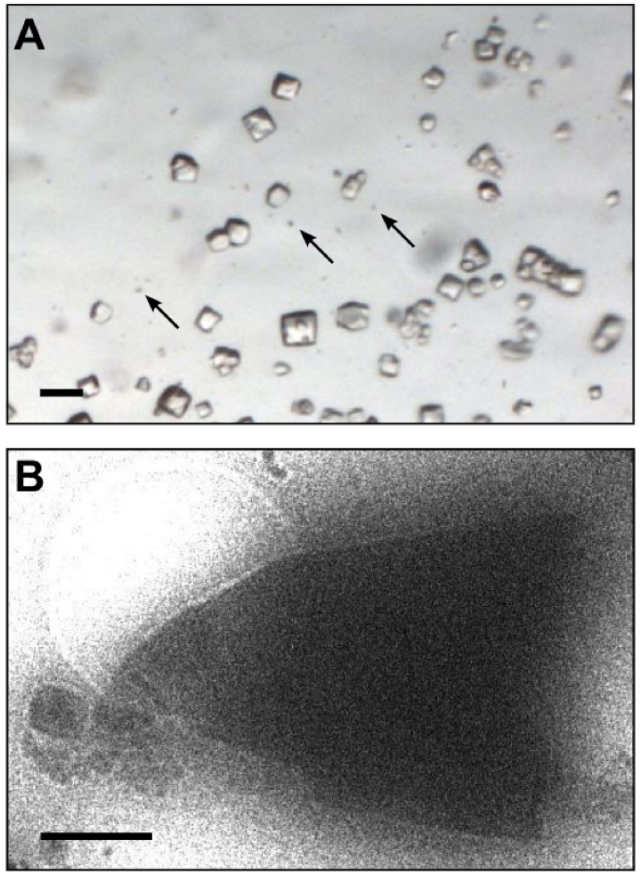

Figure 1. Images of lysozyme microrystals. (**A**) Light micrograph showing lysozyme microcrystals (three examples indicated by arrows) in comparison with larger crystals of the size normally used for X-ray crystallography. Scale bar is 50 μm. (**B**) Lysozyme microcrystals visualized in over-focused diffraction mode on the cryo-EM prior to data collection. The length and width of the crystals varied from 2 to 6 μm with an estimated thickness of ~0.5–1 μm. Scale bar is 1 μm.

DOI: 10.7554/eLife.01345.003

Critical Dose for Diffraction Imaging

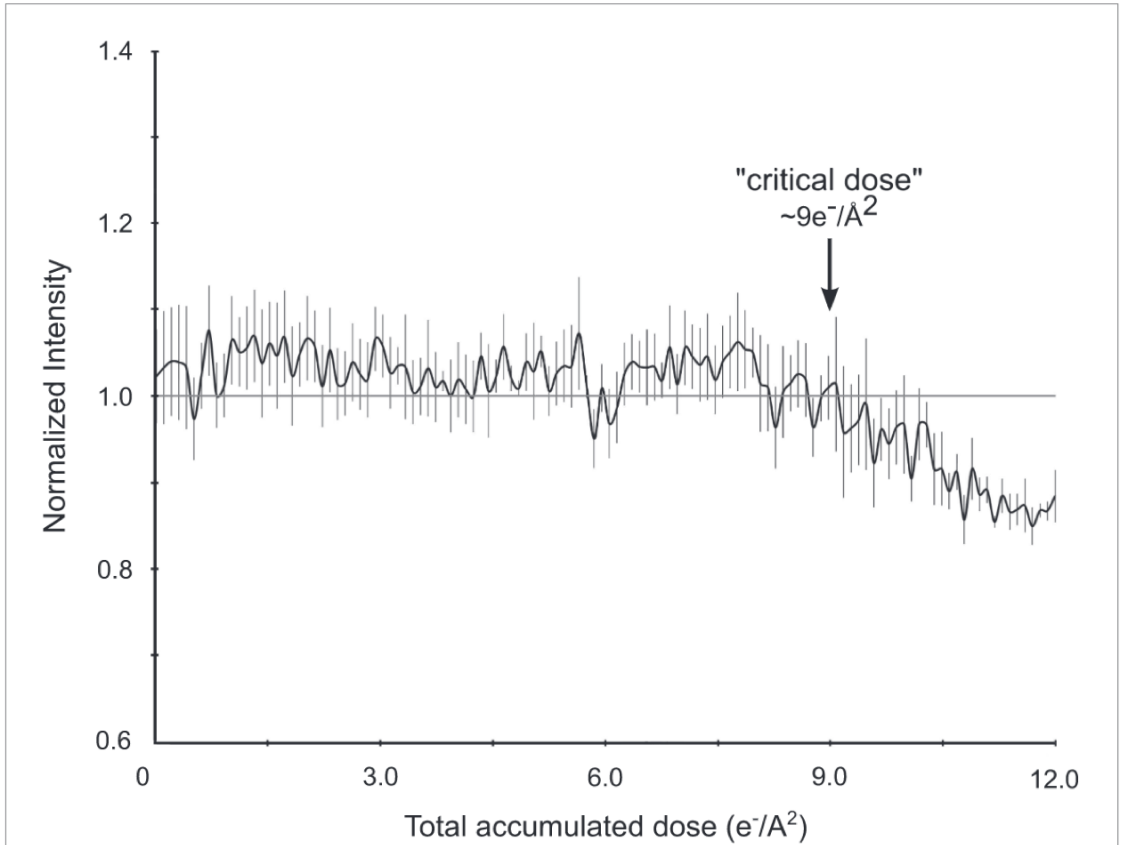

Figure 3. Effects of cumulative electron dose on diffraction data quality. A single lysozyme microcrystal was subjected to 120 sequential exposures without tilting, each of a dose of ~0.1 $e^-/Å^2$ for a total accumulated dose of ~12 $e^-/Å^2$. Normalized intensity vs total accumulated dose for three diffraction spots observed over all 120 sequential frames was plotted. A decrease in diffraction intensity becomes apparent at a dosage of ~9 $e^-/Å^2$ ('critical dose'). Bars represent standard error of the mean.

DOI: 10.7554/eLife.01345.005

Diffraction from single crystal

Video 1. An example of a complete three-dimensional electron diffraction data set from a single lysozyme microcrystal. In this example, diffraction patterns were recorded at 1° intervals from a single crystal, tilted over 47°. Cumulative dose was ~5 $e^{-}/Å^{2}$ in this example.
DOI: 10.7554/eLife.01345.006

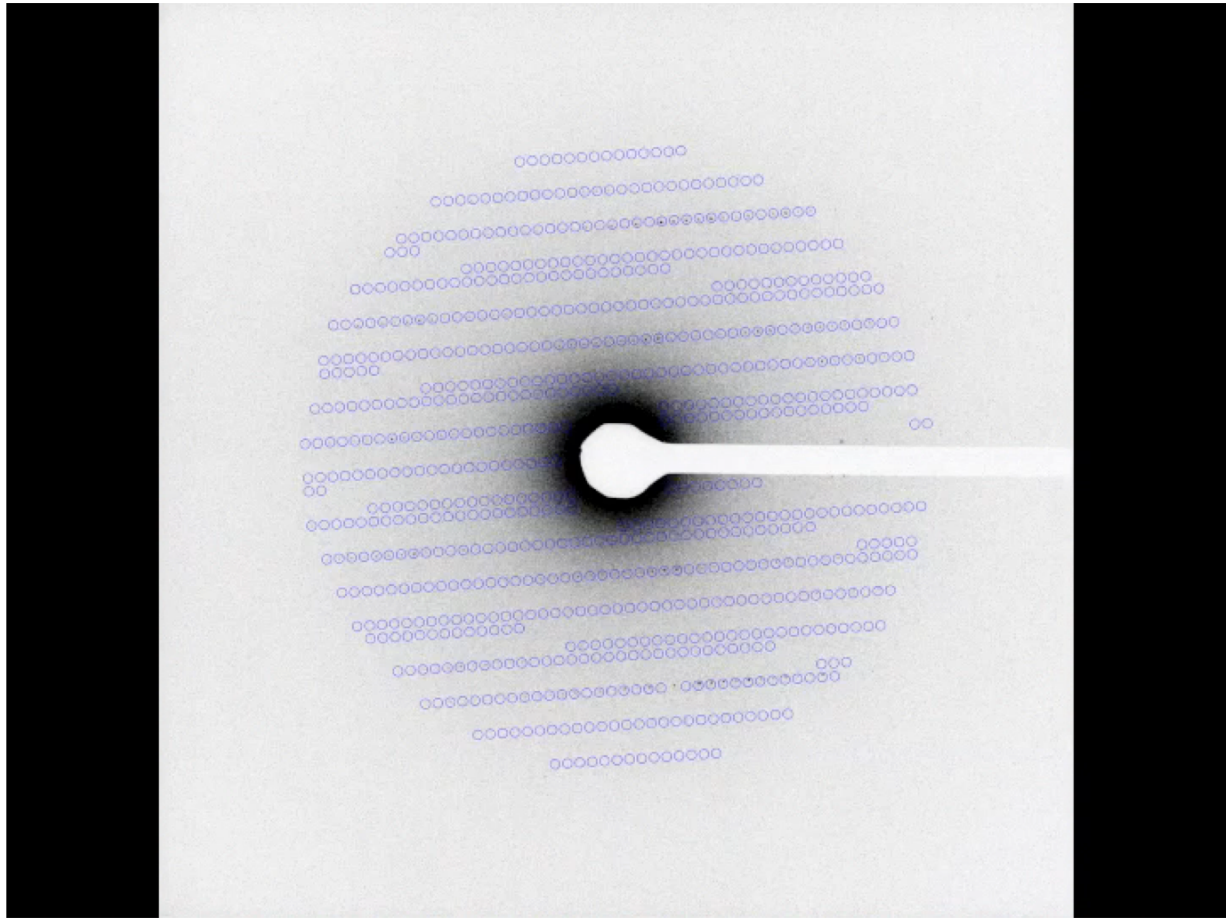

Small changes in tilt alter intensity

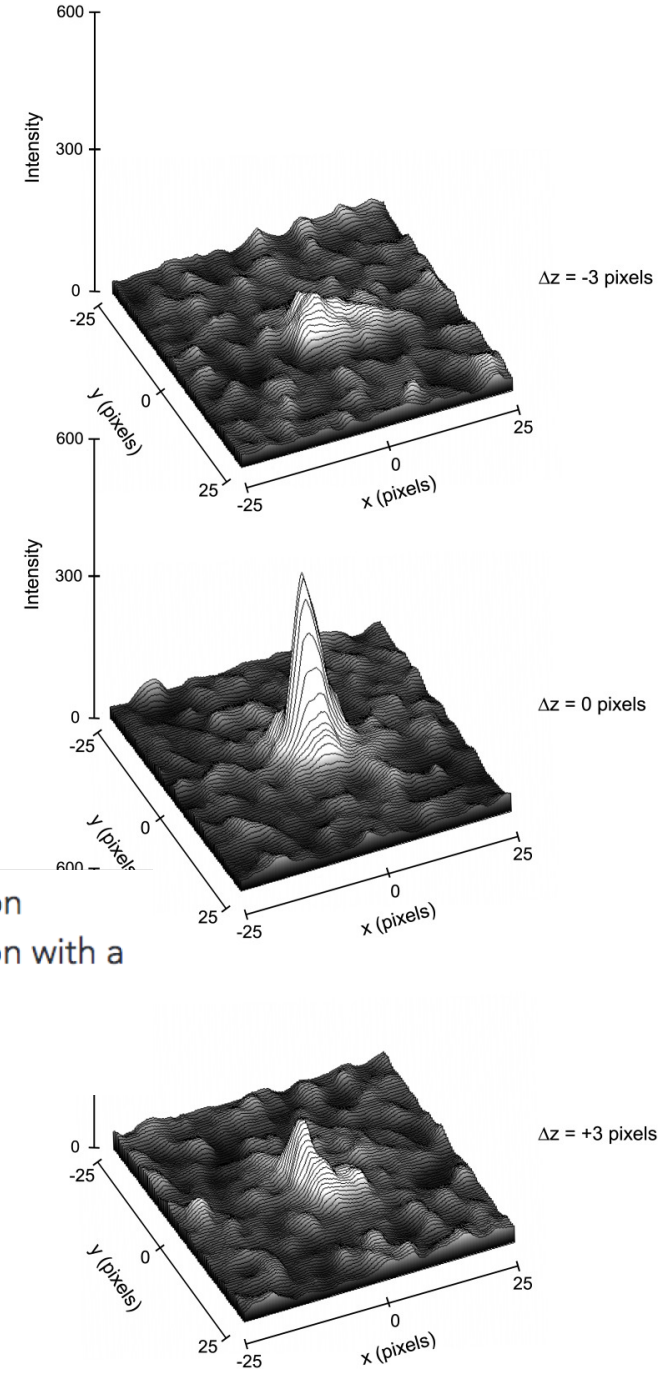

Figure 5. Three-dimensional profiles of the intensity of a single reflection over three consecutive diffraction patterns at −0.1°, 0°, and 0.1° degree tilts. The plots show the approximate dimensions of the full reflection with a width (full width at half maximum height) of 3–5 pixels in the x, y, and z direction.

DOI: 10.7554/eLife.01345.009

Better Data Collection: Continuous rotation

- Rotate stage at continuous rate (hardware or trick)
- Rotate to coordinate with exposure time
- Camera needs to be in continuous “rolling shutter” mode
- High rotation rate: increases the recorded reflection fraction on each frame
  - Too high: spot overlap
- Low rotation rate: makes weaker, high resolution reflections more visible
  - Too low: too few spots per image

Data Collection: more specifics

- To date, most MicroED data was collected on TVIPS F416 CMOS camera (4k x 4k) in “rolling shutter” mode (2k x 2k)
- Continuous readout of microscope parameters disabled
- In processing software, need to define
  - Beam Center
    - May not be center of image
    - May change due to microscope instabilities
  - Rotation rate of stage – angle and range of each frame
    - Need to record starting angle and direction (clockwise/counter-clockwise)
  - Virtual sample-detector distance
    - Calibrate from powder diffraction pattern of gold or graphite
- Conversion of movie to SMV (Super Marty View) format
  - Supported by x-ray software such as DIALS, MOSFLM, XDS

Lens magnification means physical distance to physical detector (d) is smaller than distance to virtual detector (D)

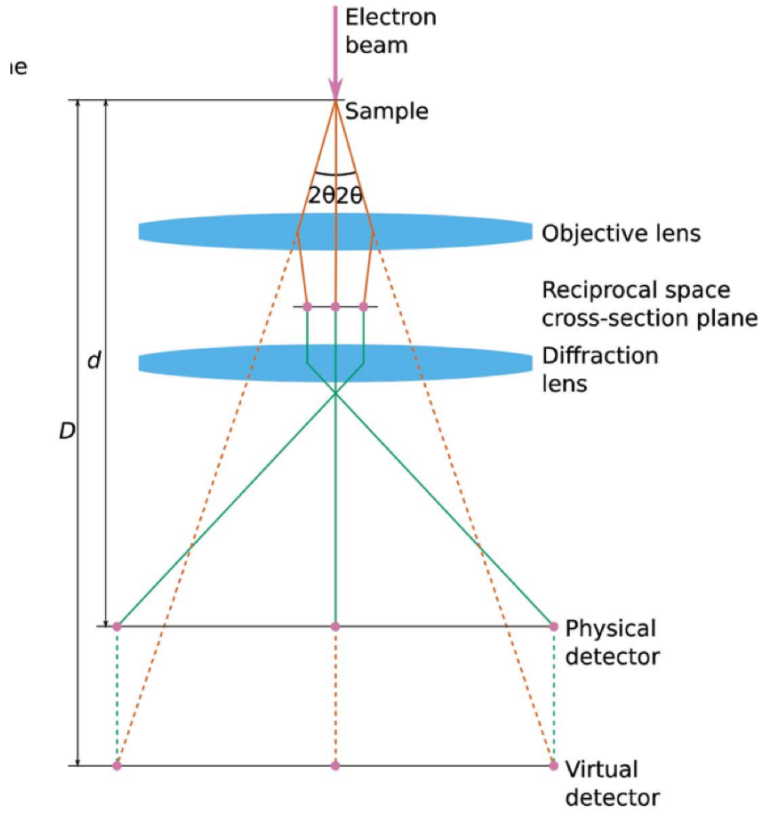

Processing Complications

- Interpretation of detector gain depends on downstream processing software
  - Ratio of variance and mean of intensities in background pixels
- Camera does not label hot or dead pixels
- Because patterns are collected at very low electron dose, even the strongest low-resolution reflections still within linear range

Indexing

- MOSFLM/AIMLESS and XDS
- Electron wavelength at 200 keV: 2.5 pm
  - Scattering angles small, Ewald sphere less curved
  - Each orientation is almost planar in reciprocal space
- 5-10 images spanning 20 degrees rotation wedge are generally enough for autoindexing
- Sample orientation calculated from the rotation rate and image timestamp
  - Large inaccuracies in initial estimate of rotation angle
- Errors in crystal orientation: absorb residual errors in the mosaicity
  - Mosaicity then acts as a sink for errors, not a model of lattice disorder

Phasing

- For most structures, phasing was done through molecular replacement
- Standard X-ray crystallography tools
- CNS, Phaser, phenix.refine, REFMAC all have electron scattering factors built in
- Ab initio phasing: has been done for small peptides
  - Need diffraction to 1.4 Å or better

Extended Data Table: Same as for x-ray crystallography

Extended Data Table 1

Statistics of data collection and atomic refinement for NACore, its fragment SubNACore, and PreNAC.

Segment	**SubNACore AVVTGVTAV**	**NACore GAVVTGVTAVA**	**PreNAC GVVHGVTTVA**
Data collection			
Radiation source	Synchrotron	Electron	Electron
Space group	C2	C2	P21
Cell dimensions			
***a*,*b*,*c* (Å)**	61.9, 4.80, 17.3	70.8, 4.82, 16.79	17.9, 4.7, 33.0
α,β,γ (°)	90, 104.1, 90	90, 105.7, 90	90, 94.3, 90
Resolution (Å)	1.85 (1.95–1.85)	1.43 (1.60–1.43)	1.41 (1.56–1.41)
Wavelength (Å)	0.9791	0.0251	0.0251
R_{merge}	0.117 (0.282)	0.173 (0.560)	0.236 (0.535)
$R_{r.i.m.}$	0.135 (0.322)	0.199 (0.647)	0.264 (0.609)
$R_{p.i.m.}$	0.065 (0.154)	0.093 (0.311)	0.185 (0.305)
$I/\sigma I$	5.2 (2.7)	5.5 (2.5)	4.6 (1.8)
$CC_{1/2}$ **(%)**	99.5 (97.8)	99.4 (92.3)	96.7(74.0)
Completeness (%)	97.9 (98.3)	89.9 (82.6)	86.9 (69.6)
Multiplicity	4.1 (4.0)	4.4 (4.3)	3.7 (3.5)
Refinement			
Resolution (Å)	1.85 (2.07–1.85)	1.43 (1.60–1.43)	1.41 (1.41–1.57)
No. reflections	470 (125)	1073 (245)	1006 (239)

*Highest resolution shell is shown in parenthesis.

Structure of Amyloid core

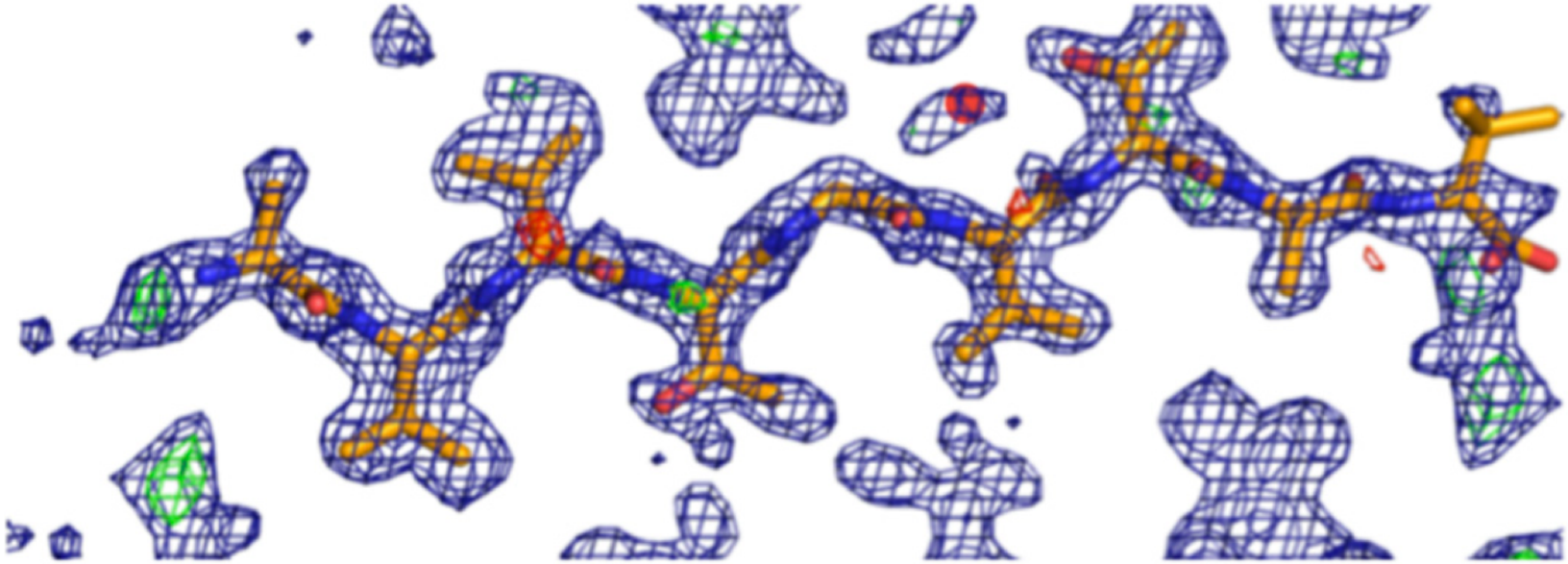

Difference density maps calculated after successful molecular replacement using the SubNACore search model clearly revealed the positions of the missing residues (positive F_o-F_c density at N and C termini corresponding to G68 and A78) and one water molecule near a threonine side chain (red circle); a second water was located during the refinement process. The blue mesh represents $2F_o$-F_c density contoured at 1.2 σ level. The green and red mesh represent F_o-F_c density contoured at 3.0 and −3.0 σ, respectively. All maps were σa-weighted[61].

2Fo-Fc Density map shows location of 5/73 protons (green)

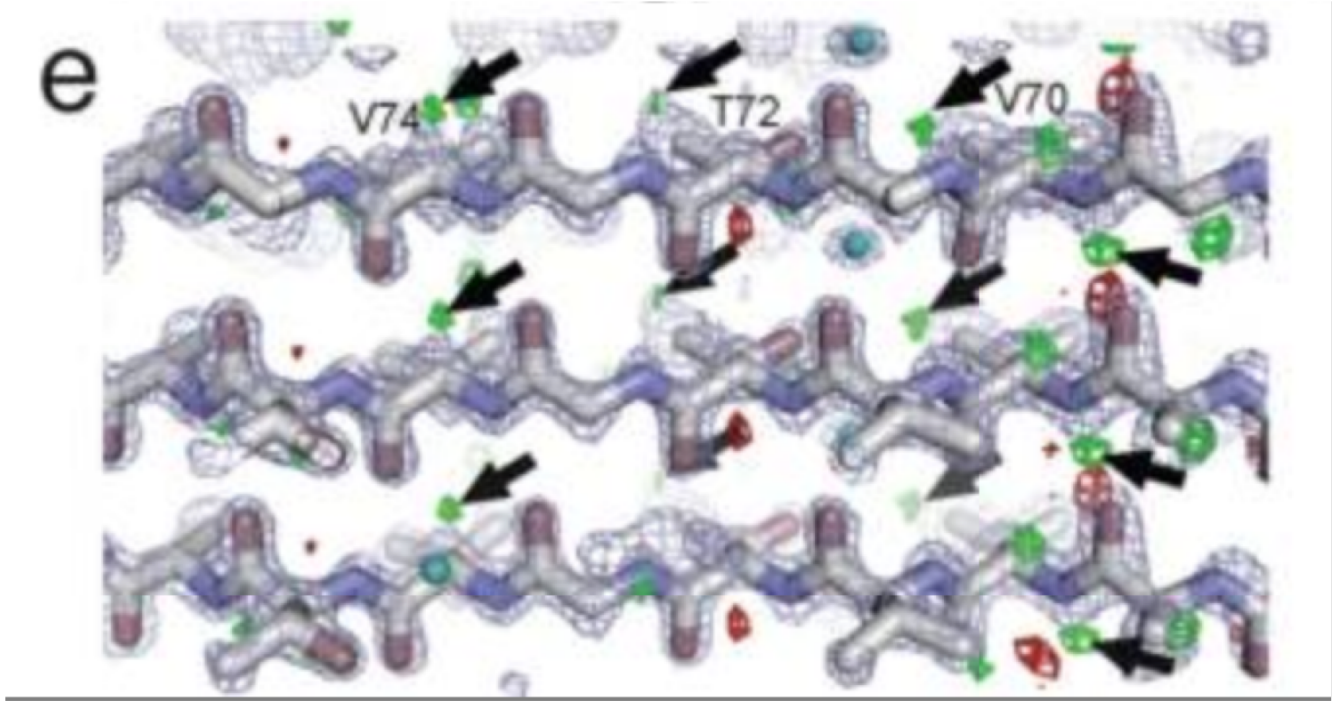

Future Directions

- Direct phasing rather than molecular replacement
  - Requires resolution 1.4Å or better
- Heavy atom derivatives?
- Use images of 3D crystals for phasing?
- Develop more accurate electron scattering factors for improved refinement

Imaging 3D crystals (Igor Nederlof, Yao Wang Li, Marin van Heel and Jan Pieter Abrahams, 2013)

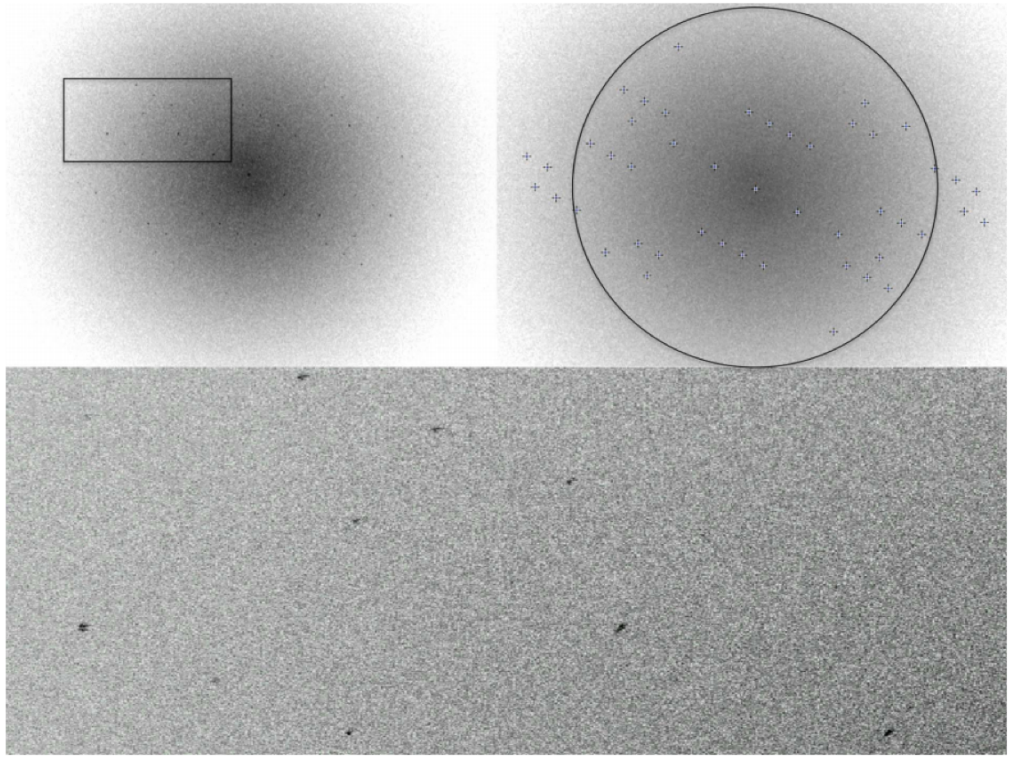

Figure 3
Top left, slightly enlarged Fourier transform of Fig. 2(*a*). Top right, Fourier transform of Fig. 2, with peak positions indicated, showing a projection of a regular three-dimensional lattice (the ring represents 4.5 Å). Bottom, detail of the top left, showing the structure of the Bragg spots.

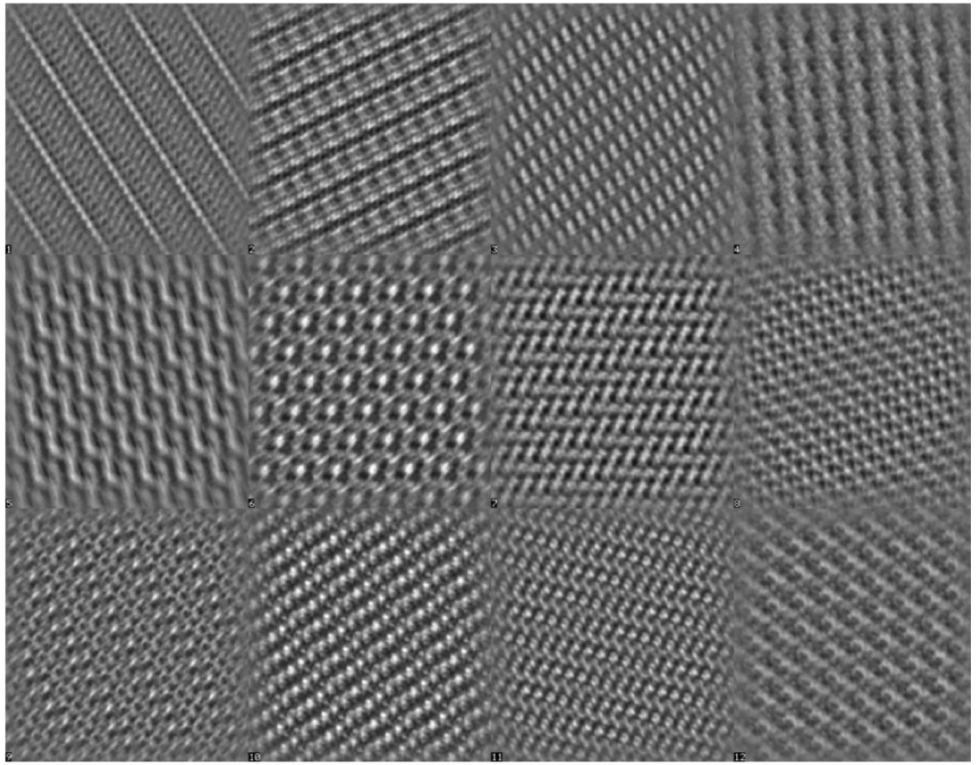

Figure 8
A dozen of the more than 200 high-resolution projection images (resolution better than 2.5 Å judging from their Fourier transforms) of different lysozyme three-dimensional nanocrystals, all in different orientations. The data were collected as in Fig. 2 and processed as described in the text.

Summary

- Advantages
  - Mid-level equipment (200 keV, FEG, CMOS detector with movie mode)
  - Alignment probably less difficult than for imaging mode
  - Highest resolution yet achieved by cryo-EM technique
  - Processing software (X-ray) mature and well understood by a large community
- Disadvantages
  - Need crystals – screening is slow
  - Crystals must be small (400 nm max thickness) and randomly oriented
  - High quality stage essential, continuous slow tilting mode needed
  - Phasing problem: molecular replacement unless quality is extremely high
  - Maybe maximum size?

Questions

References

References
[1-13]

1. Hattne, J., et al., *MicroED data collection and processing.* Acta Crystallogr A Found Adv, 2015. **71**(Pt 4): p. 353-60.
2. Iadanza, M.G. and T. Gonen, *A suite of software for processing MicroED data of extremely small protein crystals.* J Appl Crystallogr, 2014. **47**(Pt 3): p. 1140-1145.
3. Liu, S., et al., *Atomic resolution structure determination by the cryo-EM method MicroED.* Protein Sci, 2017. **26**(1): p. 8-15.
4. Nannenga, B.L. and T. Gonen, *Protein structure determination by MicroED.* Curr Opin Struct Biol, 2014. **27**: p. 24-31.
5. Nannenga, B.L., et al., *Structure of catalase determined by MicroED.* Elife, 2014. **3**: p. e03600.
6. Nannenga, B.L., et al., *High-resolution structure determination by continuous-rotation data collection in MicroED.* Nat Methods, 2014. **11**(9): p. 927-930.
7. Rodriguez, J.A., D.S. Eisenberg, and T. Gonen, *Taking the measure of MicroED.* Curr Opin Struct Biol, 2017. **46**: p. 79-86.
8. Rodriguez, J.A. and T. Gonen, *High-Resolution Macromolecular Structure Determination by MicroED, a cryo-EM Method.* Methods Enzymol, 2016. **579**: p. 369-92.
9. Rodriguez, J.A., et al., *Structure of the toxic core of alpha-synuclein from invisible crystals.* Nature, 2015. **525**(7570): p. 486-90.
10. Sawaya, M.R., et al., *Ab initio structure determination from prion nanocrystals at atomic resolution by MicroED.* Proc Natl Acad Sci U S A, 2016. **113**(40): p. 11232-1123
11. Shi, D., et al., *The collection of MicroED data for macromolecular crystallography.* Nat Protoc, 2016. **11**(5): p. 895-904.
12. Shi, D., et al., *Three-dimensional electron crystallography of protein microcrystals.* Elife, 2013. **2**: p. e01345.
13. Yonekura, K., et al., *Electron crystallography of ultrathin 3D protein crystals: atomic model with charges.* Proc Natl Acad Sci U S A, 2015. **112**(11): p. 3368-73.